NUMERICAL SIMULATION OF A FLAP-EDGE FLOWFIELD[1]

C.L. Streett
NASA Langley Research Center
Hampton, VA, USA

Abstract

In this paper we develop an approximate computational framework for simulation of the fluctuating flowfield associated with the complex vortex system seen at the side edge of a flap in a multi-element high-lift airfoil system. The eventual goal of these simulations is to provide an estimate of the spectral content of these fluctuations, in order that the spectrum of the noise generated by such flowfields may be estimated. Results from simulations utilizing this computational framework are shown.

Introduction

Sound from an aircraft induced purely by airflow not related to the engine is known as airframe noise. During approach its levels rival that of the engine, causing a threat to the successful certification of future subsonic aircraft.

NASA's Noise Reduction Program began a recent effort to study Airframe Noise in 1995, partnering with United States major airframe industries. NASA Langley's role is to determine fundamental noise source mechanisms by relating sound generation to fundamental fluid mechanics. It is important to realize that airframe noise prediction methods currently employed by industrial designers are based partly on broad-brush scaling estimates and partly on empirical data; little if any direct information regarding the actual noise generation mechanism is used, and for the most part, the details of these generation mechanisms remain unknown. Our program involves building block experiments coupled to large scale and flight tests performed at NASA Ames and industry. The work to be described below details one aspect of this effort pertaining to advanced computational tools, in particular, the tools utilized to understand the unsteady fluid dynamics associated with the high-lift system.

Prediction of Flow-Induced Noise

Although the subject of considerable study for the case of jet flows [1], the direct prediction of the noise produced by locally-separated flows on aircraft components through the use of numerical simulation has received comparatively little attention. Additionally, such flowfields tend to be rather complex in their mean, thus experimental investigations of the fluctuations occurring in these flows are also lacking. Both of these shortfalls result from the spatial and temporal resolution that would be required for a complete description of the mean and fluctuating flowfield. For example, in a companion study to this article [2], steady Reynolds-averaged Navier-Stokes (RANS) calculations are compared with experimental results for a simple part-span flap model of a high-lift system. The computation, using a well-established code, required a mesh of over 19 million grid points for adequate spatial resolution of the flowfield; these results are used in this study as a mean state for the computation of an approximate fluctuating flowfield, as will be described. Although this large computation, requiring about 50 hours of Cray C-90 CPU time, provides good spatial resolution of the steady flowfield, it is completely inadequate to accurately capture the majority of the fluctuations that are believed to generate noise in this flow. Additionally, these fluctuations are known to be broadband in frequency. Since the computational effort required to simulate unsteady phenomena is roughly proportional to the ratio of the highest-to-lowest frequencies, it is clear that the use of unsteady RANS to simulate these fluctuations is out of the question, at least for the near future, even if issues such as the calibration of the turbulence model for capturing unsteady flows could be answered.

The experimental investigation with which these steady RANS computations are compared in [2] required no less effort to achieve an adequate description of the steady part-span flap flowfield [3].

[1] This paper is declared a work of the U.S. Government

sensitive paint and five-hole probe surveys. Data from the latter will be shown in a later section.

Thus, it is clear that in order to provide some detailed estimate of the origin and frequency content of fluctuations in a complex aerodynamic flowfield such as that occurring about the high-lift system of a commercial subsonic transport aircraft, let alone directly predicting the noise generated by such a flowfield, some approximation is required. In this study, three major approximations are used to reduce the problem to a level that allows at least a rough estimate of the frequency content and directivity of the noise generated by the flow at the side edge of the flap of a high-lift system. Although approximate, these estimates are based on simulations of the true physical phenomena which generate the noise, and are of reasonable computational cost that parameter studies are possible.

This first approximation comes in the invocation of the Lighthill acoustic analogy [4]. As will be seen in the following section, this allows the combined noise generation and propagation problem, as would be solved in a so-called "direct computational aero-acoustics" simulation using the unsteady compressible Navier-Stokes equations, to be divided into a computation of the fluctuations in the near field and a separate computation of the generation and propagation of the noise. The former computation is still somewhat too large to be manageable, due to the resolution requirements discussed above, requiring further approximation. The second approximation lies in the use of the incompressible Navier-Stokes equations to simulate the near-field fluctuations. As the local Mach numbers seen in the flap-edge flowfield are generally below 0.3 for typical applications, this is considered reasonable, but the reduction in computational effort afforded by this approximation is still less than required to allow for a full simulation of the near-field fluctuations in this complex flow. In this study, therefore, the use of the "temporal" approximation is used to reduce the simulation of the full three-dimensional flowfield into a series of two-dimensional simulations; this approximation will be discussed and justified in later sections.

The use of local, approximate-but-rational numerical simulations to estimate the fluctuations in a flowfield that are expected to generate noise represents an improvement over previous studies, in that the physics of the generation of the fluctuations is not assumed *a priori* (beyond assuming that it is represented by the Navier-Stokes equations). In fact, the overarching philosophy embodied in the program Transport Program) can be employed in the prediction of any flow-induced noise. First, the steady flowfield must be understood, through a combination of detailed experiment and careful application of configuration RANS computations, using somewhat simplified building-block geometries. Next, the flowfield is examined for features that are capable of producing large-amplitude organized fluctuations of the proper scale and frequency, and approximate simulations to describe these fluctuations are carried out. Such fluctuations would reasonably be expected to be the primary noise generators in a flow, and would likely (but not necessarily) result from fundamental instabilities of the flowfield. It is well recognized that inflectional instabilities can occur even in nominally turbulent flows, such as shear layers, and result in the reorganization of steady mean vorticity into fluctuating vorticity of possibly large amplitude. The nonlinear interaction of these fluctuations, and/or the evolution of these fluctuations in a rapidly-varying mean flow, would be the mechanisms for noise generation.

Lighthill's Acoustic Analogy

What follows is a very brief and incomplete description of the fundamentals of Lighthill's acoustic analogy, in order to illustrate how the theory allows, at least conceptually, for the noise source and propagation mechanisms to be separated. The reader is referred to the original reference [4] and works by Ffowcs-Williams [5] and Lilley [6] for more complete descriptions.

The basis of the theory is an exact expression of the compressible Navier-Stokes equations. In the absence of boundaries and mean flow, this equation is:

$$\frac{\partial^2 \rho'}{\partial t^2} - c_o^2 \frac{\partial^2 \rho'}{\partial x_i^2} = \frac{\partial^2}{\partial x_i \partial x_j}\left(\rho_o u_i u_j\right) \qquad (1)$$

The LHS of the equation is clearly a linear wave equation, and depicts the propagation of density fluctuations due to sound. The RHS, which results from the nonlinear convection terms in the momentum equation, acts as a source to the medium outside the region of fluctuating flow. This source is assumed known, derived from solutions or estimates of the nearfield fluctuating flow.

In the presence of (stationary) boundaries, an additional, surface source term appears [5]:

$$\frac{\partial}{\partial x_i}\left[p_{ij}\,\delta(f)\frac{\partial f}{\partial x_j} \right]$$

where f=0 defines the surface, and p_{ij} contains the fluctuating surface pressure and viscous stresses. By asymptotic analysis, it may be shown that for smooth surfaces, this source term dominates. However, in the presence of corner or edges, current investigations in which full CAA computations are compared with acoustic analogy results indicate that the volume term must be included.

Flap-Edge Flowfield

Based on both experimental and computational studies [2][3], a fair understanding of the steady flowfield in the vicinity of the edge of a flap of a high-lift system has been gained. Clearly, the difference in lift between flapped and unflapped sections of a wing with a part-span flap will result in a trailing vortex emanating from near the flap edge, as shown in Fig 1 which depict the streamlines wrapping around the flap side edge. The details of the development of this vortex are surprisingly complex. Shown in Fig. 2 are contours of a quantity that approximates the streamwise component of vorticity, displayed in planes normal to the flap edge and chord line [3], denoted "crossflow" planes. As can be seen, surfaces of the flap creates flow around the edge. Two separation bubbles, with associated streamwise vorticity and rollup, are created at the upper and lower corners of the flap edge. The reattachment point of the side-edge vortex moves up the edge as the flow progresses down the flap, eventually reaching the upper corner. The side-edge vortex then travels over the upper corner, interacting and eventually merging with the upper-surface vortex. This leaves a single trailing vortex, which is continually fed with vorticity from the cylindrical shear layer that emanates from the lower edge corner. This mechanism of continual feed of vorticity into the vortex produces a strong jet-like flow in the core of the vortex, where streamwise velocities of over twice the freestream velocity have been measured. For this flap section, which was chosen for building-block study due to its simple geometry, the trailing vortex leaves the flap surface and is more than a vortex-diameter clear of the surface when it reaches the trailing-edge location. For other, more representative flap sections, careful RANS computations indicate that the vortex may remain in the vicinity of the surface or upper corner until reaching the trailing edge. This has implication in the amount of noise generated by fluctuations that develop in the vortex/shear-layer system.

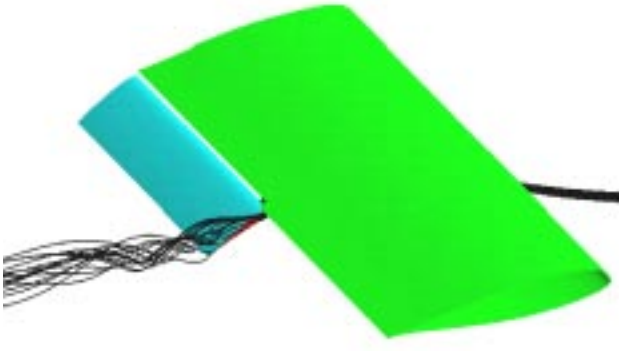

Figure 1 Streamlines in flap-edge flowfield

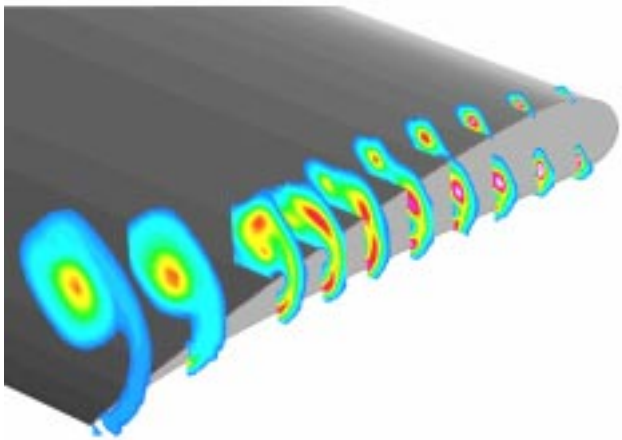

Figure 2 Contours of streamwise vorticity at flap edge

Numerical Simulation Algorithm

We wish to compute unsteady incompressible Navier-Stokes solutions in a geometry that includes the rectilinear end of the flap; both formal and *a posteriori* justifications for this temporal simulation framework

algorithm for such solutions is described in [8]; the physical domain is divided into rectangular sub-domains as required, and tensor-product Chebyshev spectral collocation of the pertinent equations is employed in each sub-domain. In Fig. 3 is shown an example of such a multi-domain discretization. Note that the corners of the geometry are isolated at corners

discretization, and do not disrupt the expected spectral accuracy. Two additional sets of sub-domain divisions are employed in the discretization in Fig. 3, which set up layers of sub-domains both above and to the right of the main computational region of interest. In these outer sub-domains, the extensively-used buffer domain technique [9] is employed to provide a non-reflecting numerical outflow boundary condition which allows passage of fluctuations that reach the boundary of the overall computational region, preventing contamination of the interior solution.

The "interface" conditions, the discrete equations which are used to couple the solutions across coinciding sub-domain boundaries, are specific to the particular equations being solved; for second-order equations, strong enforcement of $\mathbf{C^1}$ continuity has been found to perform well, as well as various flux-balance conditions [8].

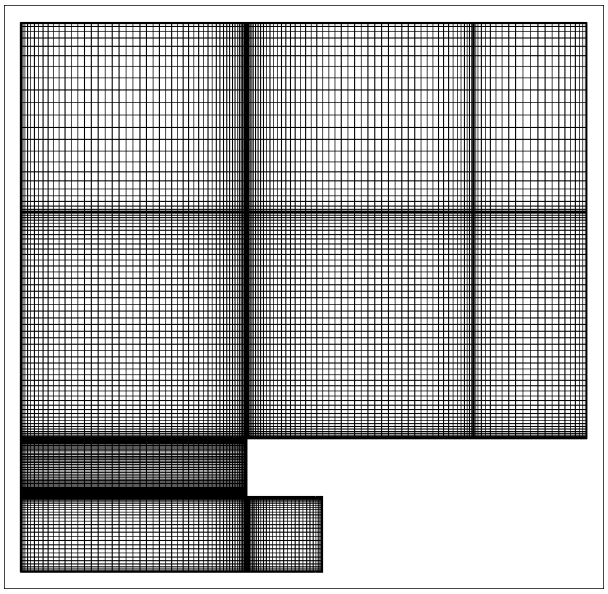

Figure 3 Multi-domain discretization of crossflow plane at flap edge

A simple time-splitting algorithm is used to advance the incompressible Navier-Stokes equations in time. This robust and accurate method, described in detail in [10], is easily employed in this multi-domain context, as it reduces the solution of the Navier-Stokes equations to solution of a sequence of Helmholtz and Poisson equations. Solutions of these equations fit easily in the above-mentioned interface scheme, and are carried out very rapidly on a computer using a variant of tensor-product diagonalization [9]. The resulting simulation code is so efficient that all of the SGI Indigo^2 desktop workstation, and results have been obtained in the past using a 133-MHz Pentium PC.

Results

Cylindrical Shear Layer Instability

In [2] is described the results from a series of high-resolution steady RANS computations, for flow about a generic part-span flap configuration which has been extensively used in a number of experimental investigations of flap-edge noise [11][12][3]. We utilize those solutions here as mean flowfields for disturbance simulations, interpolating the RANS solutions onto the spectral multi-domain discretization topology described earlier. These interpolations are carried out in planes that are taken to be roughly normal to the axis of the vortex system. In order to study the growth of disturbances of particular frequencies, a small amount of local forcing is applied in these simulations, at a point on the lower surface of the flap that is a significant distance from the lower corner. The forcing is applied as a short region of oscillatory suction and blowing, and careful examination of the unsteady flowfield showed little if any influence of location and size of the forcing region on the overall results. This is an indication of the strength of the instability mechanism at work in this flowfield, and leads us to conclude that the details of what provides the initial energy to these fluctuations in the actual flowfield is probably irrelevant; what matters is the amount of amplification that the inflectionally-unstable flowfield provides, as a function of frequency. The flowfield details that influence this instability, the strength, location, and thickness of the cylindrical shear layer, for instance, are functions of the configuration and loading. Comparisons of simulation results with surface fluctuating pressure and farfield noise data for the experiment of [12] are forthcoming.

For a plane located at a streamwise station of roughly 10%-flap chord, the mean flowfield consists of distinct side- and top-corner vortices, with the side-edge reattachment point at about mid-thickness. The shear layers over these vortices are relatively thin, so higher frequency disturbances are expected to dominate. In Fig. 4 is shown contours of the mean vorticity, and snapshots of the disturbance vorticity for forcing at three different frequencies. These frequencies are taken in the model scale of [12], and the contours displayed are all normalized with respect to the maximum from each simulation. Each simulation required about 4 hours of SGI workstation time to reach statistical steady state.

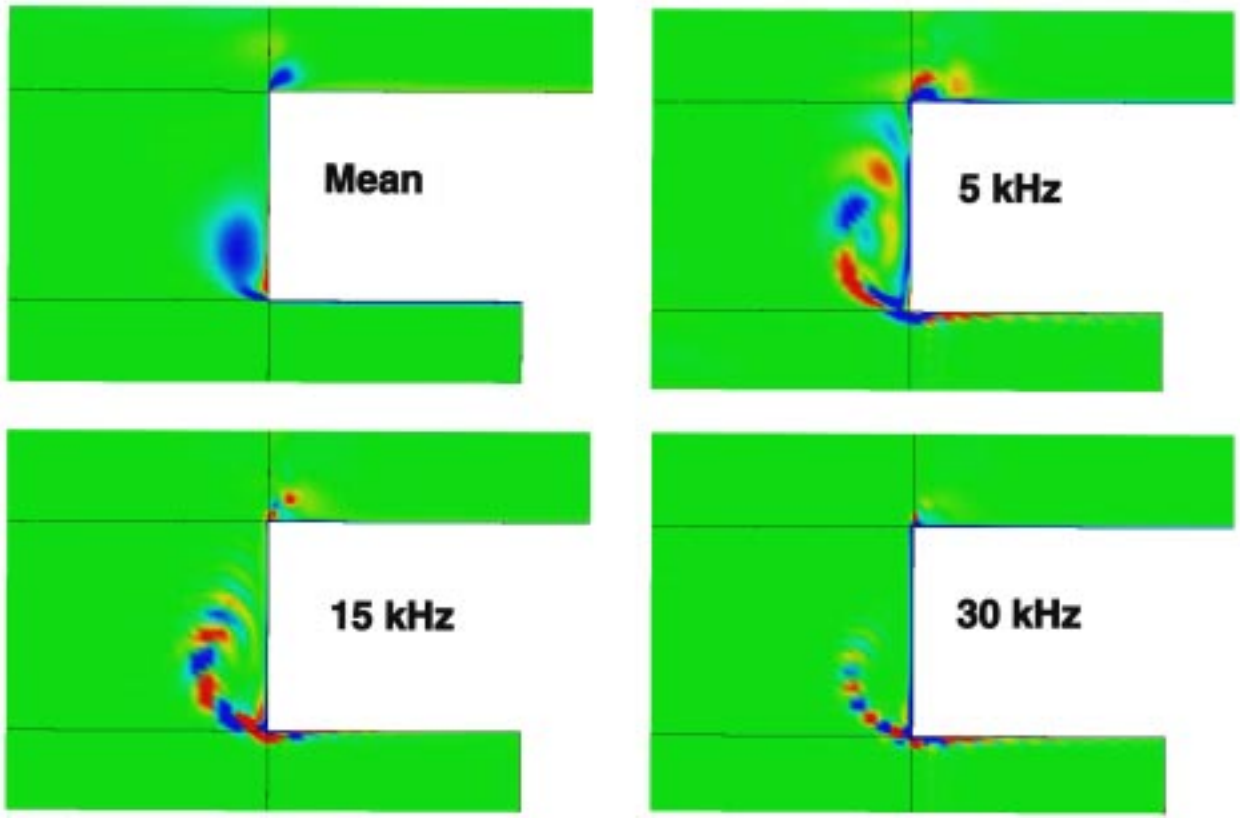

Figure 4 Contours of mean and disturbance vorticity, 10%-flap chord station

Near the lower corner, fluctuation strength as measured by disturbance vorticity magnitude is greatest for the 15 kHz forcing, with 30 and 5 kHz disturbances being 30 and 39% smaller, respectively. At a point in the shear layer near mid-thickness, the lowest (5 kHz) disturbance dominates, with 15 and 30 kHz disturbances 59 and 62% smaller.

In a plane at approximately 50% flap chord, the side-edge and top vortices have merged, and the cylindrical shear layer / vortex system is well established. Contours of mean and disturbance vorticity are shown in Fig. 5, again with three model frequencies of 5, 15, and 30 kHz forcing. The instability of the cylindrical shear layer is quite apparent, with the 5 kHz disturbances persisting with significant magnitude even as they are convected over the vortex. Maximum disturbance vorticity magnitudes in the shear layer are roughly equal for the three frequencies, demonstrating the broadband nature of the instability.

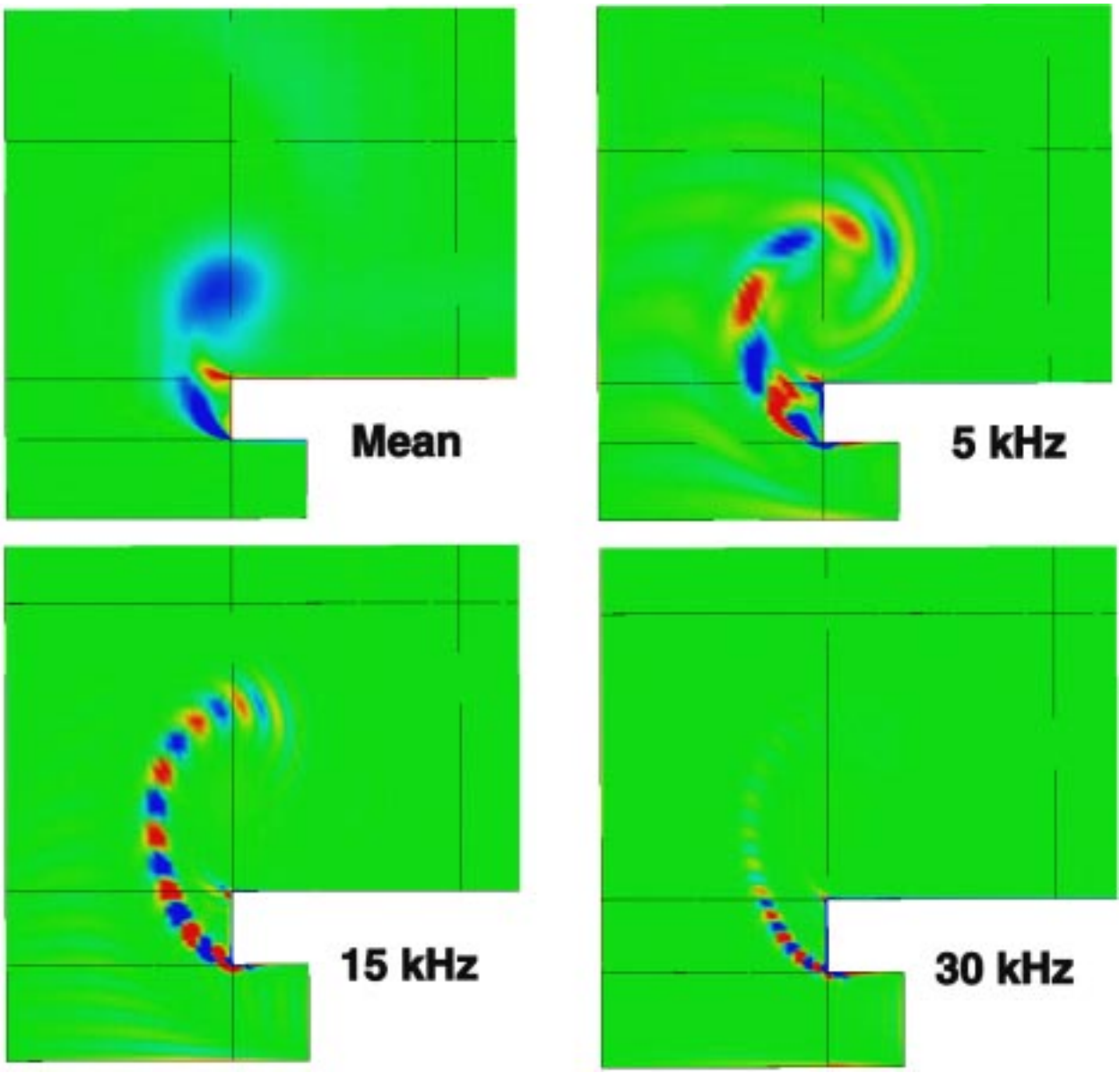

Figure 5 Contours of mean and disturbance vorticity, 50%-flap chord station

As mentioned above in the discussion of the Lighthill acoustic analogy, the fluctuating surface pressure is of interest in regard to the prediction of noise produced by a fluctuating flowfield. Contours of $\log_{10}(|p'_{surf}|)$ are shown in Fig. 6, displayed with the time coordinate as the third spatial dimension. Apparent in the figure is the change in location of concentration of fluctuating surface pressure moving from side edge to top surface with frequency decreasing; this is expected from the disturbance vorticity contours of Fig. 5. It is believed that concentration of fluctuating surface pressure near geometric singularities such as corners is of particular importance in noise generation.

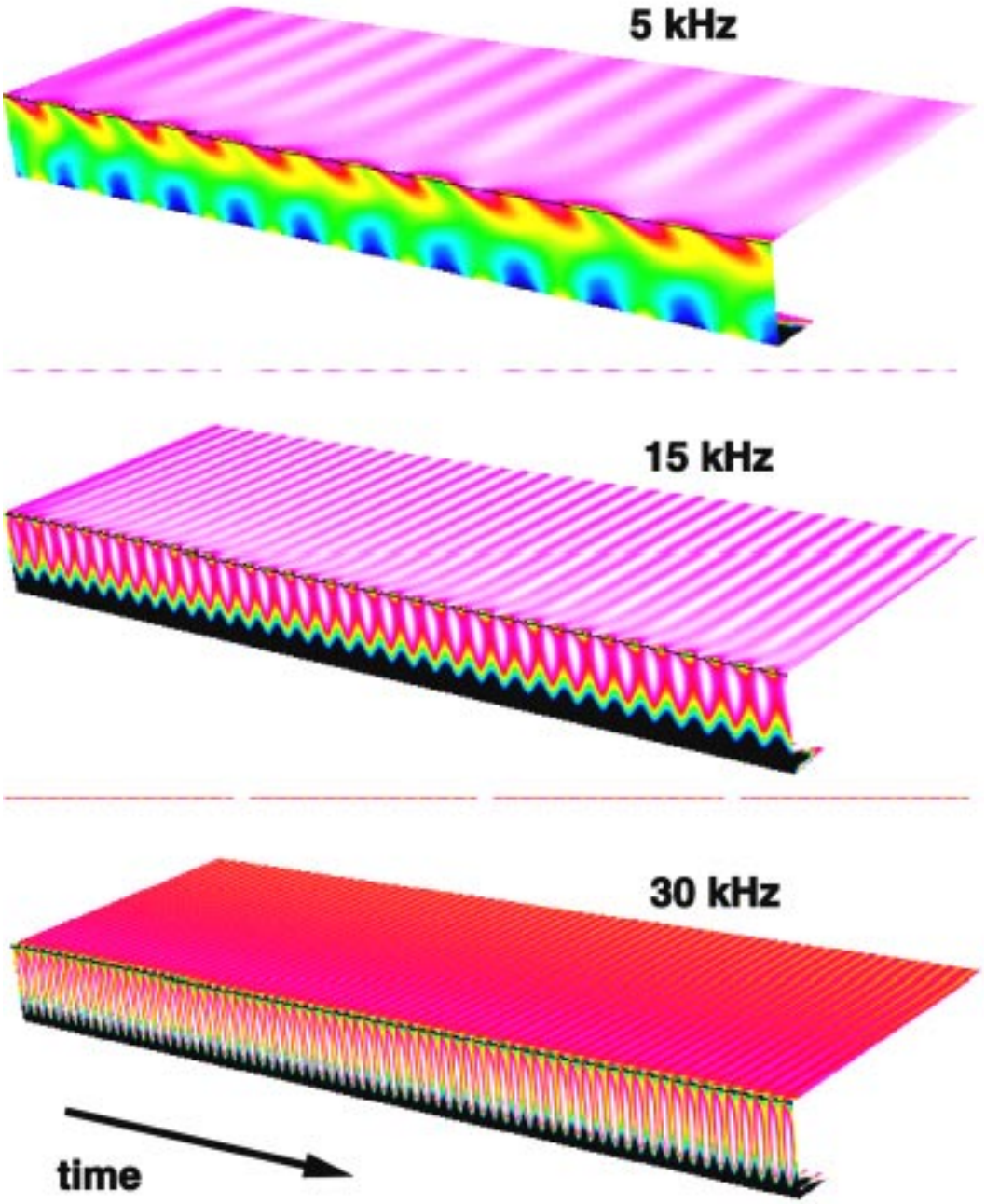

Figure 6 Contours of $\log_{10}(|p'_{surf}|)$

Vortex Instability

In the above simulations, it is assumed that the disturbances have no variation in the direction normal to the crossflow plane that is cut from the RANS solution. While this is a reasonable assumption for the instabilities that result from the cylindrical shear layer, it is conjectured that instabilities should exist also in the shear of the vortex itself, especially in vortex. Further, the disturbances resulting from this vortex instability should have significant oscillation in the streamwise direction. Assuming that the spatial scale of such oscillation is small compared with the scale of variation in the streamwise direction of the mean flow, then we can apply the additional *ansatz* that these oscillation are homogeneous in that direction in the simulation. For the following simulations,

where α is a prescribed streamwise wavenumber parameter. The full three-dimensional RANS solution, interpolated onto a crossflow plane as before, is taken as the mean state, and the (complex) equations are discretized in the crossflow plane and time advanced as before.

With this assumption, the parameter space to be explored now has two parameters: frequency and streamwise wavenumber, with the results shown earlier corresponding to the case $\alpha=0$. Results from this study are as yet incomplete, but it has been found for the most part that the shear-layer instabilities are maximally amplified for $\alpha=0$. However, there exists a separate family of instabilities, associated with the conjectured vortex-instability mechanism; the high, corresponding to wavelengths on the order of ¼ to ½ of the vortex diameter. The dominant frequency band of these disturbances is considerably lower than that for the shear-layer instability; in model frequencies, the shear-layer instability band was roughly 5 to 30 kHz, whereas the vortex instability band is about 1 to 10 kHz. In Fig. 7 is shown a comparison of snapshots of disturbance vorticity for the two disturbance modes, using broadband forcing for each simulation; the vortex mode has a streamwise wavelength of 1/3 of the vortex diameter. Note that the vortex disturbance has a ring-like structure. This is more clearly discernable in Fig. 8, in which isolevel surfaces of disturbance vorticity are shown for these same modes.

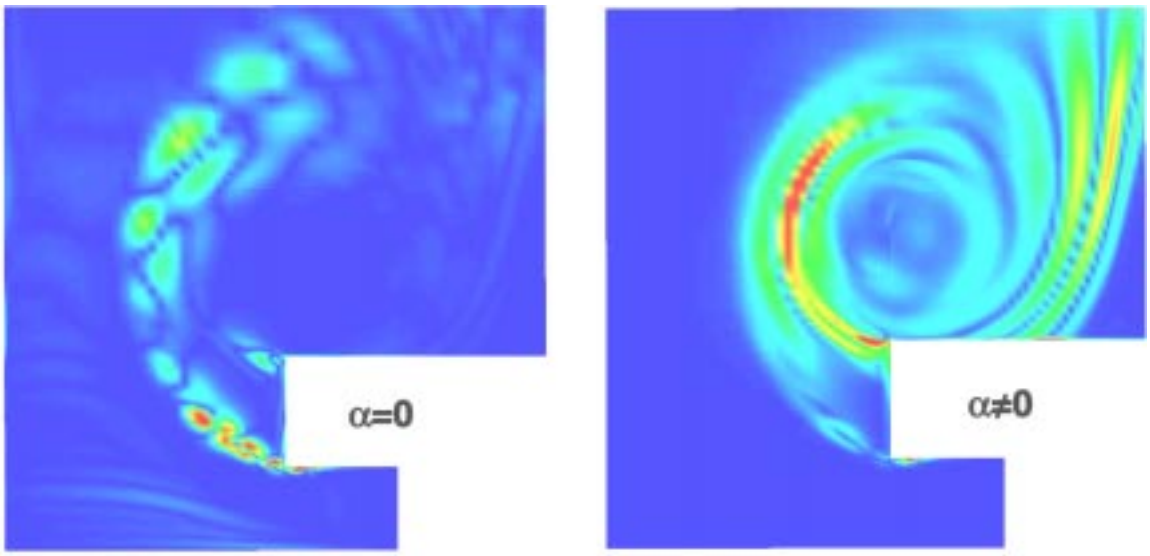

Figure 7 Disturbance vorticity snapshots, shear-layer and vortex instability modes

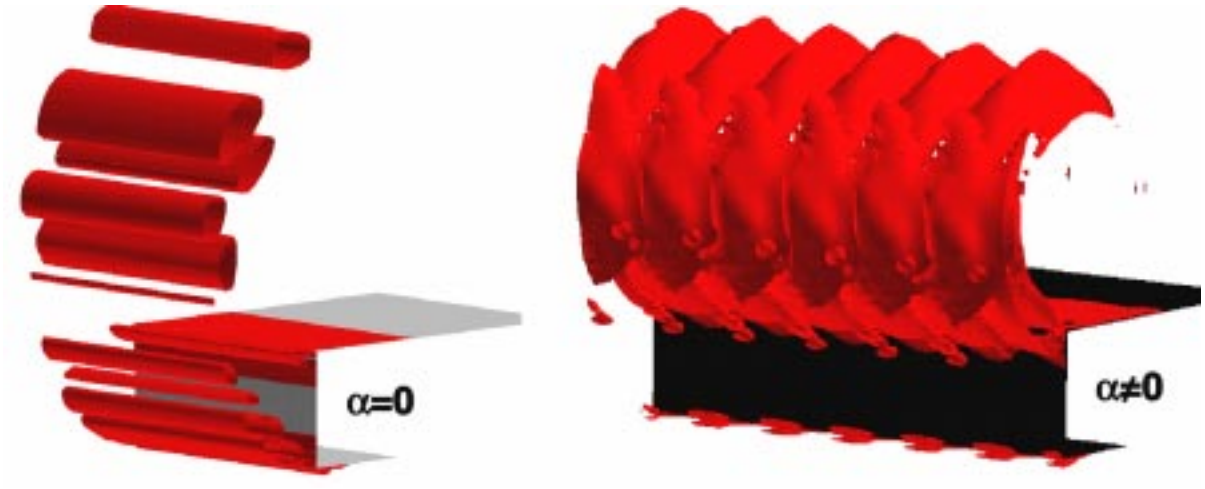

Figure 8 Isolevel surfaces of disturbance vorticity, shear-layer and vortex instability modes

These vortex disturbance modes have implication in the generation of noise, for flap configurations for which the vortex remains in proximity to the flap surface all of the way to the trailing edge; as noted above, realistic flap sections frequently show this behavior. As these disturbances convect past the trailing edge, they would be expected to have considerable amplitude and be quite coherent in the spanwise direction; thus it would be expected that a significant amount of locally-enhanced trailing-edge noise would result. While initial experimental observations indicate that this is indeed the case, comparisons with experimental data are ongoing.

Noise Generation by Shear-Layer Instability

In an attempt to test whether the fluctuations predicted by the above method are related to the noise generated by a flap-edge flowfield, the RHS of Eq. 1 (the so-called Lighthill stress tensor) was computed for a number of single-frequency simulations at the 50% flap-chord station shown in Fig. 5. Contours of the Lighthill stress tensor are given in Fig. 9, from the 15kHz simulation shown in Fig. 5. Note that the strongest concentration of this quantity occurs near the corner where the cylindrical shear layer originates; this is due to the rapidly-changing amplitude and spatial wavenumber of the disturbance in that region, resulting from the strong variation in shear-layer thickness in that region.

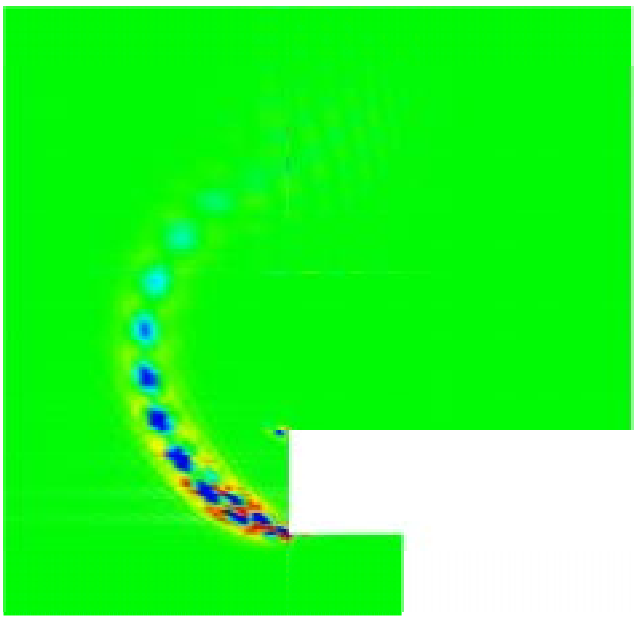

Figure 9. Contours of Lighthill stress tensor, 15kHz simulation.

The resulting acoustic field was then computed using a high-order accurate wave equation solver, forced by the computed Lighthill stress tensor; the finite-thickness flap-edge geometry was approximated by way of a conformal mapping to the infinite half-plane. Results for three frequencies are shown in Fig. 10, in terms of constant-phase contours, which show the resulting acoustic wave pattern, and in terms of contours of 20log(mag(ρ')), which gives an indication of directivity. Each contour level in the latter display is 5 dB. Note how the directivity pattern rotates with frequency, from stronger upward radiation

frequency, to a primarily downward pattern with several irregularities for the highest frequency.

One may choose a convenient location in the acoustic field at which to interrogate a sequence of simulations over a range of frequencies, and thus obtain a representative spectrum of the noise produced by the cylindrical shear-layer mechanism. Results for the point (0, -10), i.e., ten edge-thicknesses straight down from the edge, are labeled in Fig. 11 as "SPL". Note the strong peak in radiated noise at about 8 kHz, the flattening of the spectrum from about 14 to 35 kHz, and the rapid falloff beyond that point.. These results are compared with the quantity $20\log(<T_{ij}>)$, which shows the former behaviors but not the falloff. This indicates that the higher-frequency fluctuations, while still strong, are not efficient generators of noise. This is potentially because these small wavelength disturbances are not strongly distorted on their own scale by the rapidly-growing mean shear layer. Such rapid distortion is the only way in which linear disturbances with subsonic phase speed can scatter energy into modes that propagate at sonic speed.

Finally, one may compare the "SPL" results shown above with experimental spectra. Results from both [12] and [13] are shown in Fig. 12, compared with the above computations. Recall that the simulations, being linear, are without amplitude reference, and may be shifted for overall fit to the data. Note that surprisingly good agreement is obtained, all the more surprising when one reviews the assumptions which lead to the computational result: the assumption that the fluctuations in this complex three-dimensional nominally-turbulent flow may be represented by a modest-Reynolds number laminar DNS, linearized about a single plane of the mean state, and conducted in the temporal framework. While just a single result justify the hypotheses that 1) dominantly-inviscid instabilities are the driving fluctuations in this flowfield, 2) the temporal framework can predict the dominant features of these disturbances in the region in the flowfield which matters most in terms of noise generation, and 3) there is a concentrated region along the chord of the flap from which most of the noise emanates, as indicated by acoustic phased-array results [12]. [13].

Conclusions

Demonstrated in this paper is a computational framework to predict the spectral content of fluctuations in the flowfield near the side edge of a flap in a multi-element high-lift system. The framework is heuristically justified by comparison with high-resolution steady RANS solutions of the complex multi-vortex system; these RANS solutions are then utilized as mean flowfields within which unsteady disturbances are simulated. Simulations show two basic families of disturbance modes: the first is associated with instability of the cylindrical shear layer, which overlies the side-edge separation in upstream stations, and feeds the trailing vortex in downstream stations. The second family of disturbance modes is associated with instabilities of the vortex and its jet-like core flow, and possesses significant oscillatory structure in the streamwise direction. When the results from the simulations are fed into a Lighthill acoustic analogy prediction of the generated sound, preliminary results indicate surprisingly good agreement with experiment.

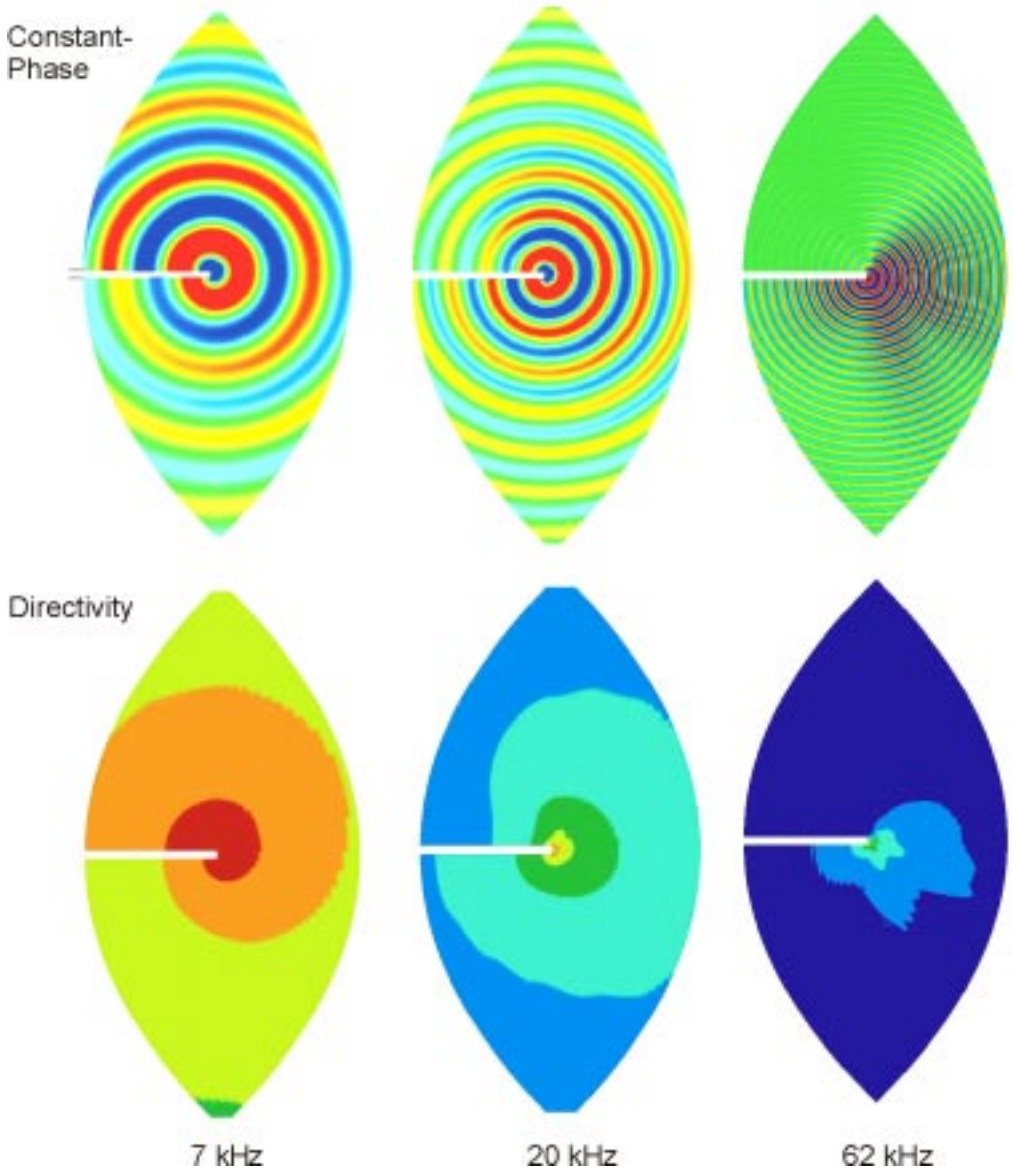

Figure 10. Wave and directivity patterns from acoustic computation.

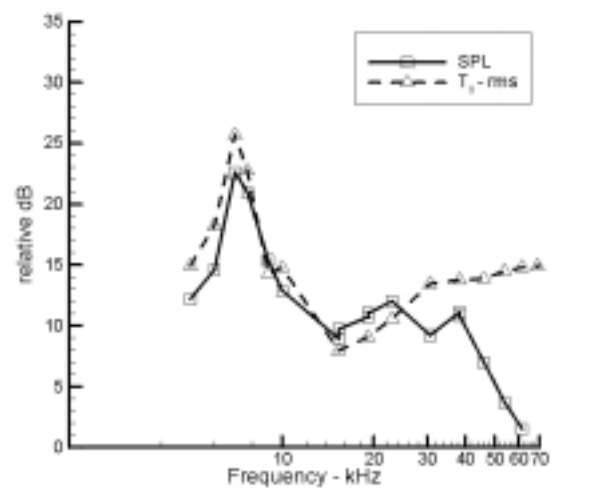

Figure 11. Comparison of amplitude of Lighthill stress tensor and radiated sound.

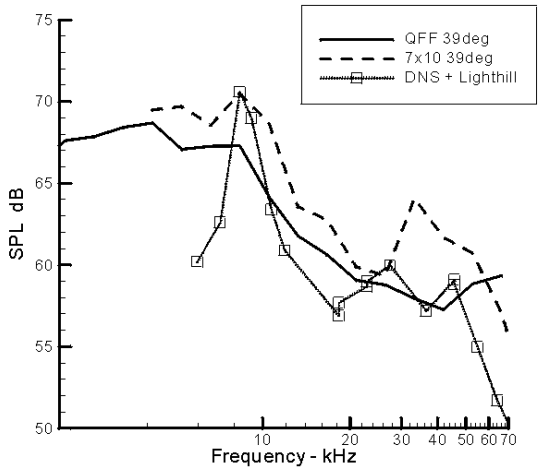

Figure 12. Comparison of predicted noise with experimental data.

References

1. Morris, P.J., Wang, Q., Long, L.N., and Lockard, D.P., "Numerical Predictions of High-Speed Jet Noise," AIAA Paper 97-1598, May, 1997.

2. Khorrami, M.R., Singer, B.A., and Radeztsky, R.H., "Reynolds Averaged Navier-Stokes Computations of a Flap Side-Edge Flow Field," AIAA Paper 98-0768, Jan. 1998.

3. Radeztsky, R.H., Singer, B.A., and Khorrami, M.R., "Detailed Measurements of a Flap Side-Edge Flow Field," AIAA Paper 98-0700, Jan. 1998.

4. Lighthill, M.J., "On Sound Generated Aerodynamically; I. General Theory," *Proceedings of the Royal Society of London*, Series A, Vol. 211, pp. 54-587, 1952.

5. Ffowcs-Williams, J.E., and Hawkins, D.L., "Sound Generation by Turbulence and Surfaces in Arbitrary Motion," *Philosophical Transactions of the Royal Society of London*, Vol. 264, No. A 1151, pp. 321-342, May 1969.

6. Lilley, G.M., "On the Noise from Air Jets," AGARD CP 131, pp. 13.1-13.12, 1973.

7. Streett, C.L., "Numerical Simulation of Fluctuations Leading to Noise in a Flap Edge Flowfield,", AIAA Paper 98-0628, Jan. 1998.

8. Macaraeg, M.G., and Streett, C.L., "Improvements in Spectral Collocation Discretization through a Multi-Domain Technique," *Appl. Numer. Math.* Vol. 2, pp. 95-108, 1986.

9. Streett, C.L., and Macaraeg, M.G., "Spectral Multidomain for Large-Scale Fluid Dynamic Simulations," *Int. J. Appl. Numer. Math.*, Vol. 6, pp. 123-140, 1989.

10. Streett, C.L., "Two Spectral Collocation Algorithms for the Incompressible Navier-Stokes Equations with Two Non-periodic Directions," *Proceedings of the First International Conference on Industrial and Applied Mathematics*, 1987.

11. Storms, B.L., Takahashi, T.T., and Ross, J.C., "Aerodynamic Influence of a Finite-Span Flap on a Simple Wing", SAE Paper 951977, Sept. 1995.

12. Meadows, K.R., Brooks, T.F., Humphreys, W.M., Hunter, W.H., and Gerhold, C.H., "Aeroacoustic Measurements of a Wing-Flap Configuration," AIAA Paper 97-1595, May 1997.

13. Storms, B. L., Ross, J. C., Horne, W. C., Hayes, J. A., Dougherty, R. P.,Underbrink, J. R., Scharpf, D. F., Moriarty, P. J., "An Aeroacoustic Study of an Unswept Wing with a Three-Dimensional High-Lift System," NASA TM 112222, Feb. 1998.